Flexible Electromagnetic Functional Fibers with Synergistic Dual-Loss Mechanisms: Achieving Ultra-Broadband Absorption and Mechanical Robustness

Yaoyao Li[a], Wanli Zhou[b], Shiyi Zhou[a*], Huan Zeng[c], Daixi Gong[a], Yanzhuo Tan[c], Mengjin Jiang[c*]

[a] *College of Materials and Chemistry & Chemical Engineering, Chengdu University of Technology, Chengdu 610059, P. R. China*

[b] *High-Tech Organic Fibers Key Laboratory of Sichuan Province, Chengdu, P. R. China*

[c] *College of Polymer Science & Engineering, Sichuan University, Chengdu 610065, P. R. China*

**Corresponding author*

E-mail address: zhoushiyi06@cdut.edu.cn, memoggy@126.com.

Fig. S1. Digital photograph of CB suspension that has been stored for 5 days.

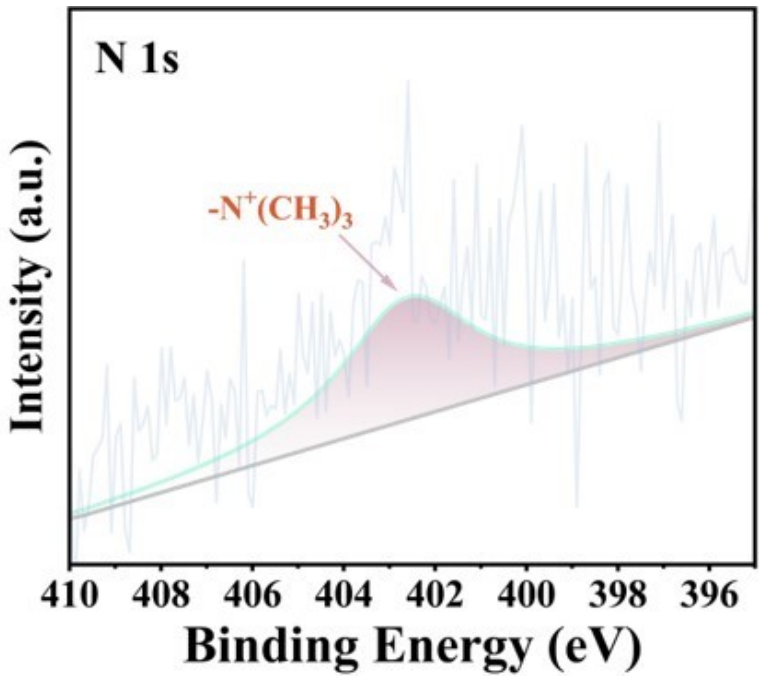

Fig. S2. High-resolution XPS spectra of CB@CTAB-OP-10: N 1s.

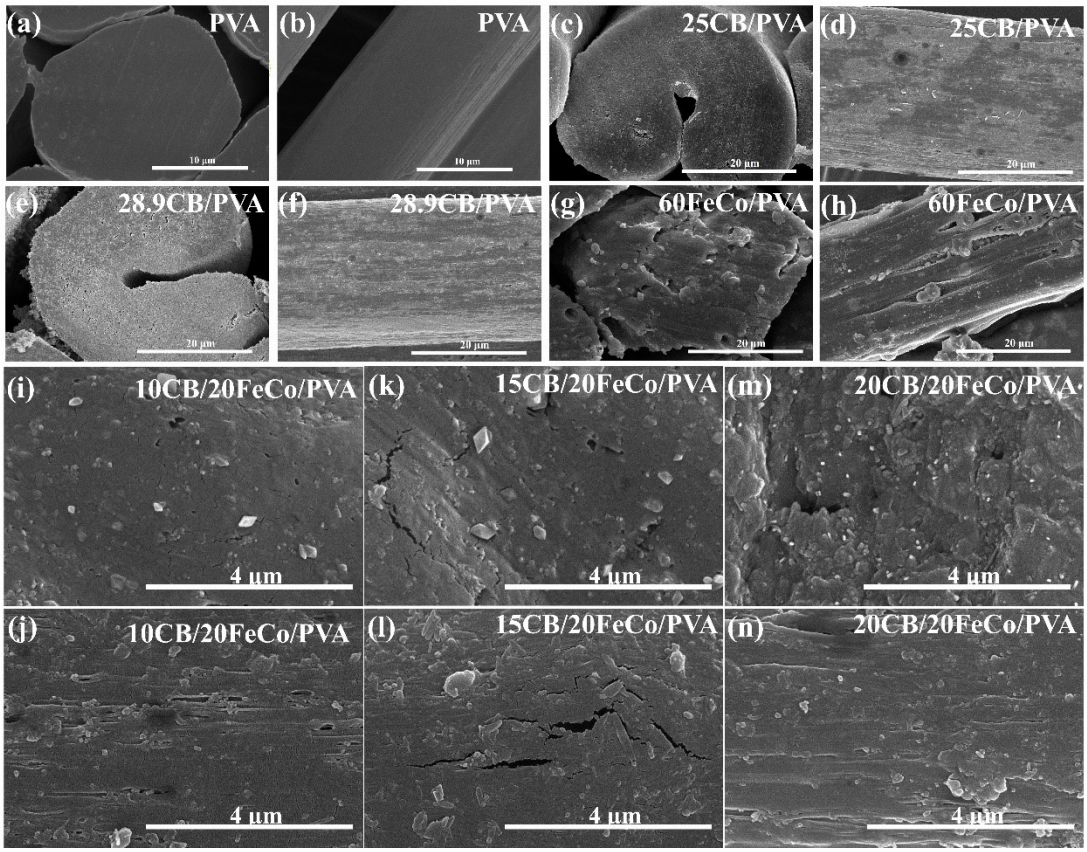

Fig. S3. SEM image of fibers, (a) and (b) PVA, (c) and (d) 25CB/PVA, (e) and (f) 28.9CB/PVA, (g) and (h) 60FeCo/PVA, (i) and (j) 10CB/20FeCo/PVA, (k) and (l) 15CB/20FeCo/PVA, (m) and (n) 20CB/20FeCo/PVA.

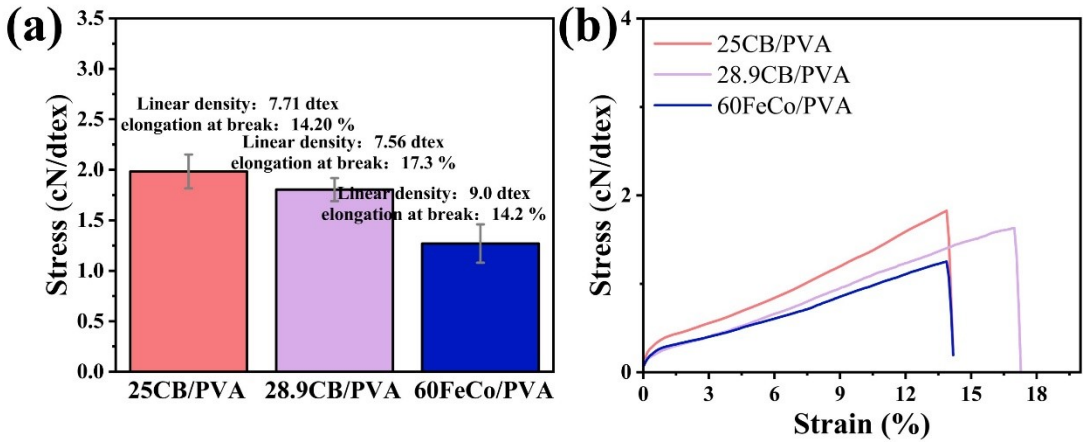

Fig. S4. (a) Tensile strength and (b) stress-strain curve of fibers.

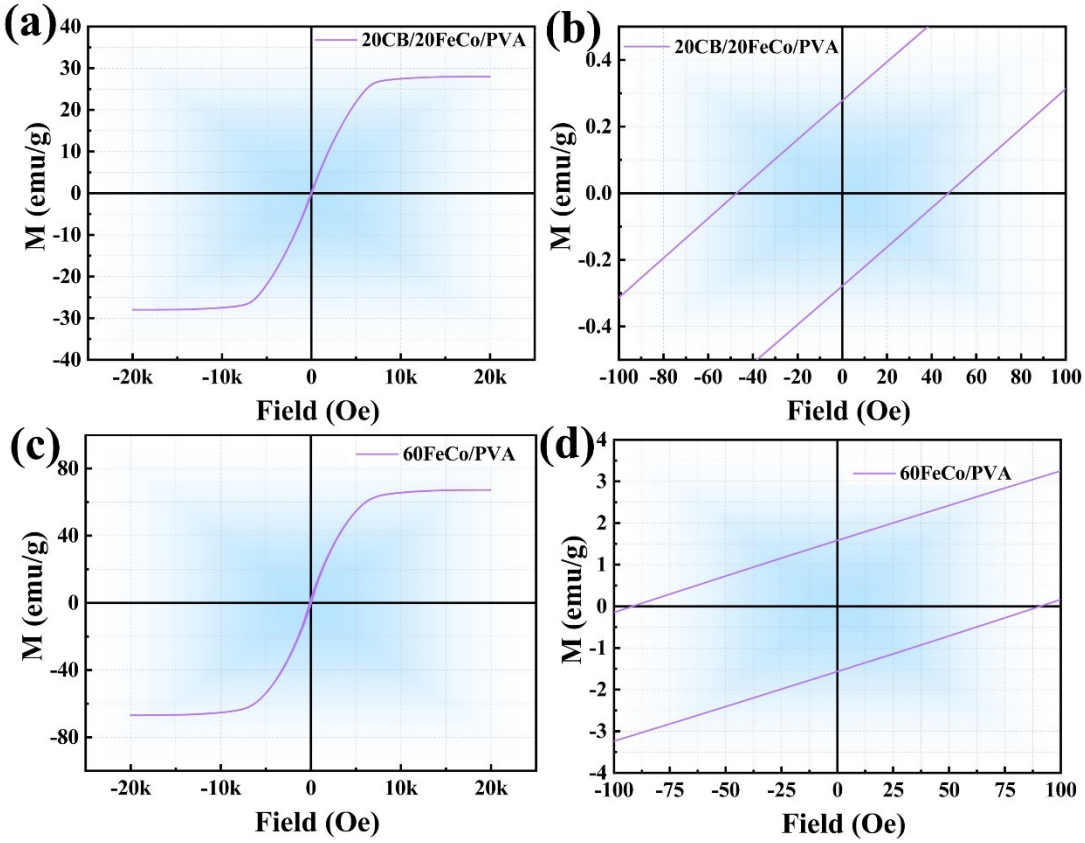

Fig. S5. Magnetic hysteresis loops: (a) 20CB/20FeCo/PVA, (c) 60FeCo/PVA, and the corresponding enlarged hysteresis loops: (b) 20CB/20FeCo/PVA, (d) 60FeCo/PVA.

Fig. S6. 20CB/20FeCo/PVA fiber: (a) Digital photographs of as-spun fibers. (b) Fibers after hot stretching treatment. (c) Physical sample of 19 cm × 19 cm non-woven fabric. (d) Physical sample of non-woven fabric after multiple folds.

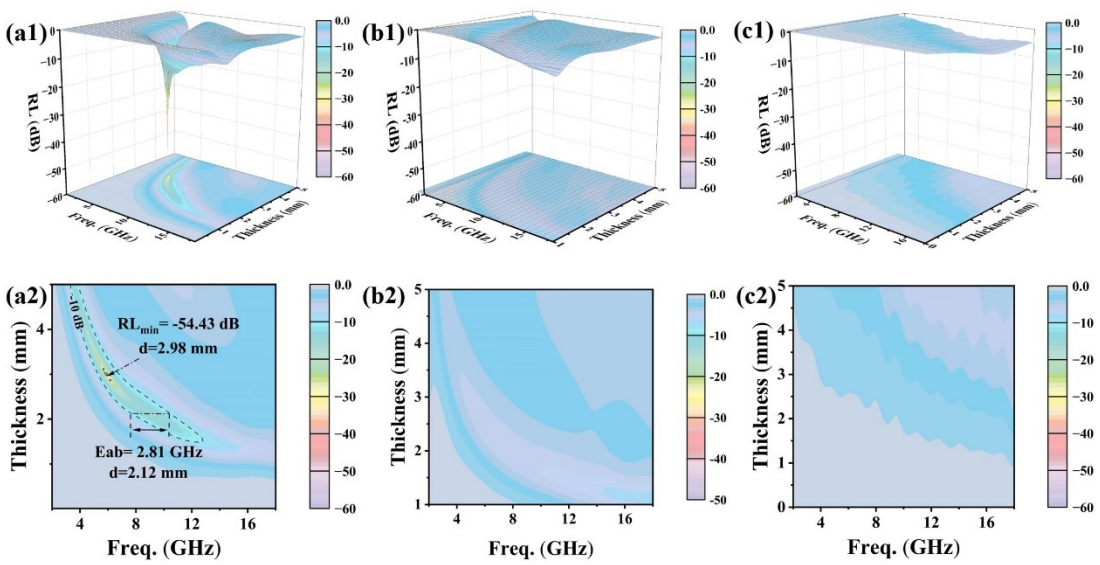

Fig. S7. Reflection loss (*RL*) value of electromagnetic function: (a) 25CB/PVA, (b) 28.9CB/PVA, (c) 60FeCo/PVA.

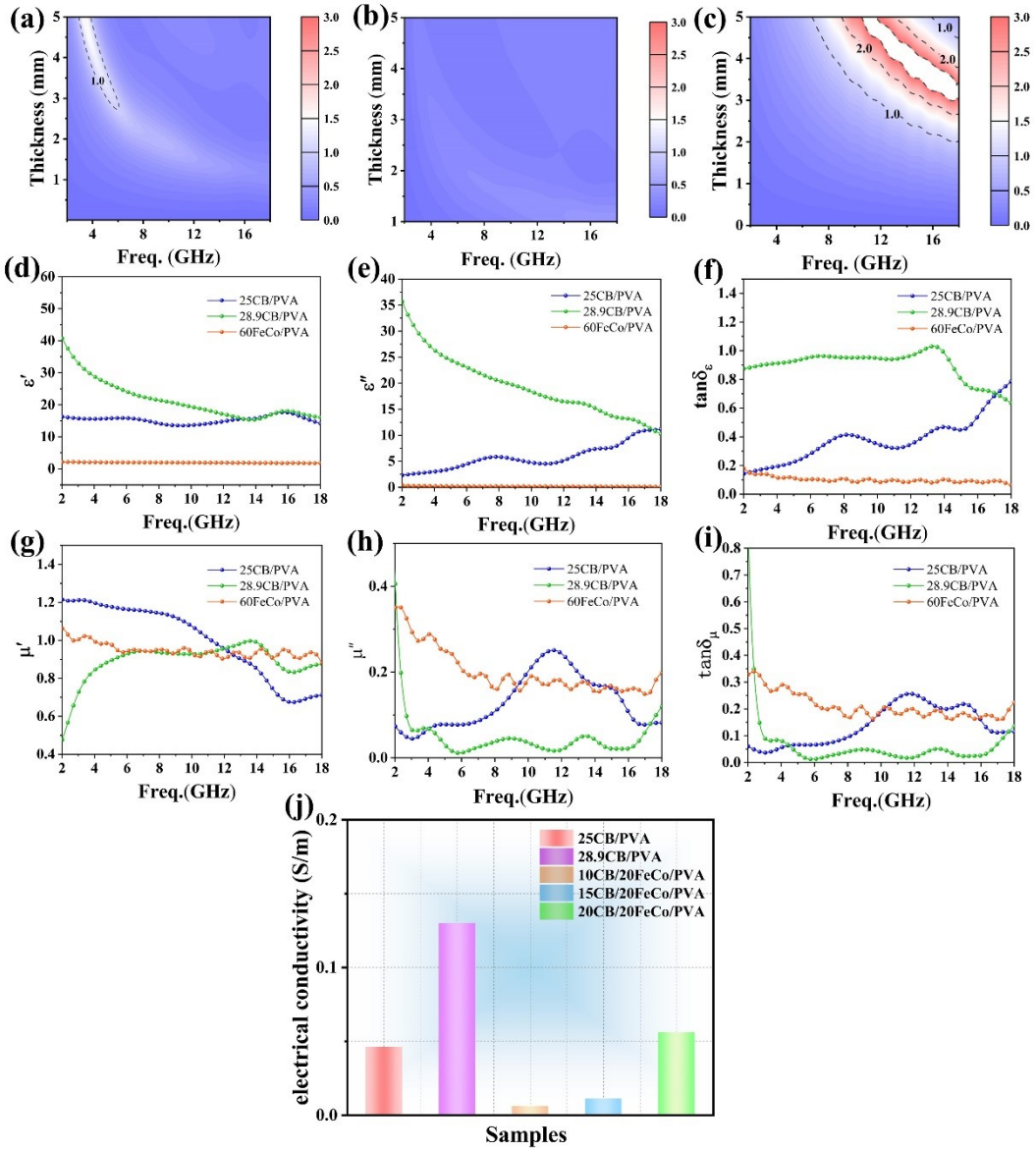

Fig. S8. A 2D color image of the $|Z_{in}/Z_0|$ value for electromagnetic functional fibers: (a) 25CB/PVA, (b) 28.9CB/PVA, (c) 60FeCo/PVA. The real part (d) and imaginary part (e) of complex permittivity for fibers. The real part (g) and imaginary part (h) of permeability for fibers. (f) $tan\delta_{\varepsilon}$ and (i) $tan\delta_{\mu}$ of fibers. (j) Electrical conductivity of composite fibers.

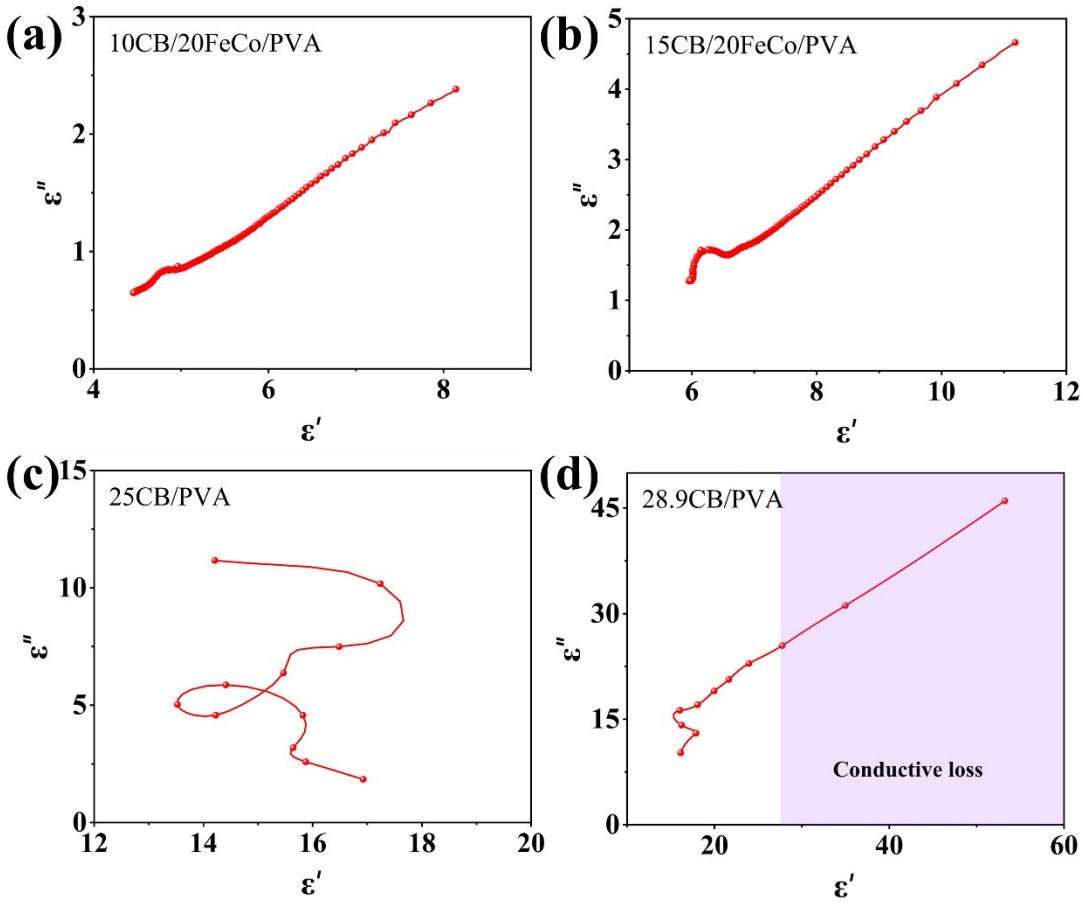

Fig. S9. The ε' vs ε'' relationship curves for 10CB/20FeCo/PVA (a), 15CB/20FeCo/PVA (b), 25CB/PVA (c), and 28.9CB/PVA (d).

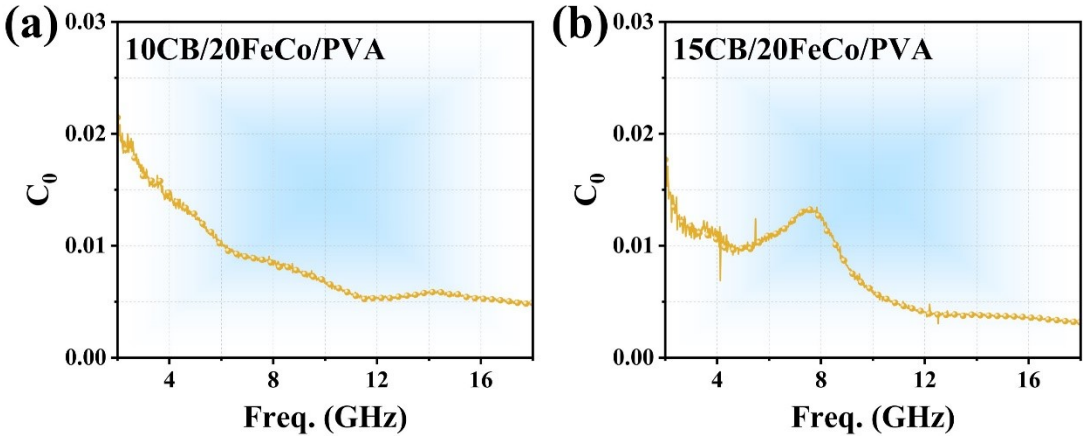

Fig. S10. The $C_0 = \mu''(\mu')^{-2}f^{-1}$ of 10CB/20FeCo/PVA (a) and 15CB/20FeCo/PVA (b).

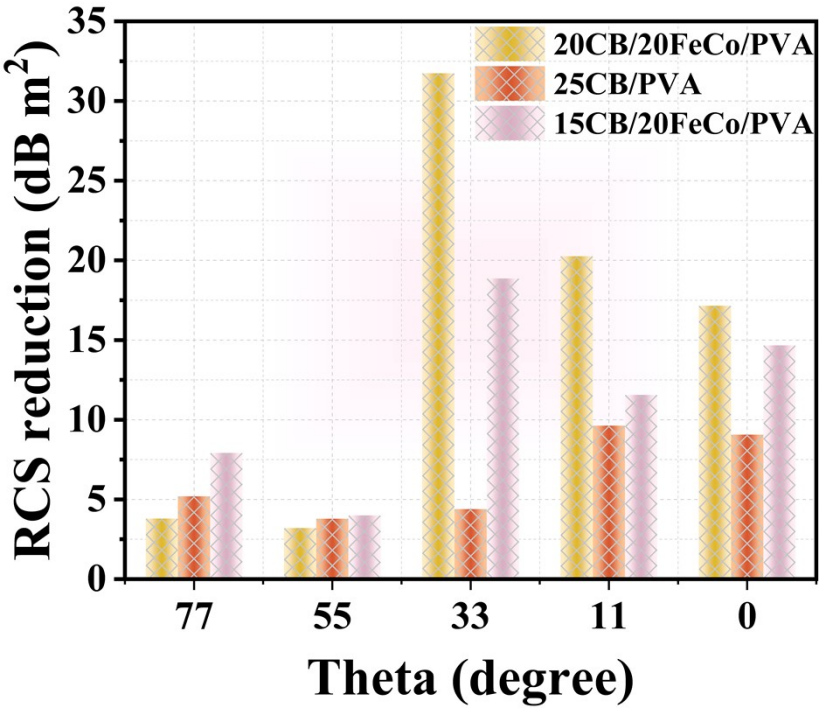

Fig. S11. RCS reduction effect of composite removal with PEC.

Table S1.

Comparison of electromagnetic wave absorption performance of 20CB/20FeCo/PVA with other materials.

Sample	Thickness/ mm	RL_{min}/ dB	Thickness/ mm	Bandwidth/ GHz	References
C@FeCoNi-60	3.00	-46.40	3.00	3.35	1
NiCo@g-C_3N_4	2.00	-35.63	2.00	4.80	2
VFT2h/MF/PPy	3.35	-39.20	2.55	5.60	3
SiCN-Fe0.5	1.50	-22.68	1.50	4.50	4
40wt.%SiCnw	1.30	-35.20	1.30	1.80	5
HPPy	3.60	-44.50	3.60	5.40	6
SiCN	2.00	-31.10	2.00	4.60	7
20CB/20FeCo/PVA	2.55	-44.36	1.83	5.70	**This work**

References

[1] Y. Wu, Q. Sun, L. Yun and J. Ge, Polym. Compos., 2025, **46**, 15782-15794.

[2] S. Hu, Y. Zhou, M. He, Q. Liao, H. Yang, H. Li, R. Xu and Q. Ding, Mater. Lett., 2018, **231**, 171-174.

[3] H. Han, Z. Lou, Q. Wang, L. Xu and Y. Li, Adv. Fiber Mater., 2024, **6**, 739-757.

[4] X. Guo, F. Xiao, J. Li, H. Zhang, Q. Hu, G. Li and H. Sun, Ceram. Int., 2021, **47**, 1184-1190.

[5] J. Kuang, T. Xiao, X. Hou, Q. Zheng, Q. Wang, P. Jiang and W. Cao, Ceram. Int., 2019, **45**, 11660-11667.

[6] H. Ren, T. Li, H. Wang, Z. Guo, T. Chen and F. Meng, Chem. Eng. J., 2022, **427**, 131582.

[7] F. Xiao, H. Sun, J. Li, X. Guo, H. Zhang, J. Lu, Z. Pan and J. Xu, Ceram. Int., 2020, **46**, 12773-12781.